Dual Stable Point Model

of Muscle Activation and Deactivation

Ching-Ping Chou

Blake Hannaford

University of Washington

Department of Electrical Engineering

FT-10

Seattle, Washington 98195

1995

19970717 145

Abstract: Two dynamic models of muscle activation and deactivation based on the concepts of ion transport, reaction rates, and muscle mechanics are proposed. Storage release and uptake of calcium by the sarcoplasmic reticulum, and a two-step chemical reaction of calcium and troponin are included in the first model. This is a concise version of the complex chemical reactions of muscle activation and deactivation in sarcoplasm. The second model is similar to the first, but calcium-troponin reactions are simplified into two nonlinear rates functions. Due to these nonlinear dynamics, the second model can explain the catch-like enhancement of isometric force response. Simulation results which match experimental data are shown. Also, two new phenomena which need further experiment to verify are predicted by the second model.

Introduction

Many attempts have been made to understand the processes by which the nervous system generates the proper activation signals to effect controlled movements. Among the factors which determine these control signals are, the intended movement trajectory, the intended sensitivity to perturbations during the movement, and the dynamics and history of the muscles and limb. This paper focuses on nonlinear dynamic features of the generation of muscle force which are relevant to the control of fast movement. The eventual goal is the incorporation of more accurate activation models in studies of human movement such as Hannaford and Stark [1985], [1987], Hannaford, Kim, Lee, and Stark [1986], and Hannaford [1990].

Many aspects of the control of muscles are dynamically complicated and non-linear. In generation of torques about a joint, the CNS can make use of a muscle through two mechanisms, recruitment of a proportion of the motor units in the muscle, and modulation of the force generated by each motor unit. Within a given motor unit, the nervous system must regulate the activation of muscle force through pulse rate coding of action potentials delivered to the neuro-muscular junction. The nature of this coding and the constraints it puts on the neural control methods depend in turn on the dynamics of the activation response to action potential sequences.

Experimentalists have addressed this problem in several muscles in the cat by artificially stimulating the motor neuron axon to deliver action potentials to the motor unit (Burke et. at. [1970], Gurfinkel and Levik [1974]). It is assumed that the regenerative, all-or-none properties of the axon (Hodgkin & Huxley [1952]) cause the action potentials received by the motor unit to be indistinguishable from those arising naturally from the motoneuron soma itself. Thus the only free variables in this stimulation experiment are the arrival times of the action potentials, in particular, their relative interarrival times. The dependent variable is the isometric force generated by the motor unit.

The theory of linear systems enables the analyst to predict the response of a linear, time-invariant, (LTI) system to any series of impulses from the response of the system to a single impulse. Unfortunately for this simple method of analysis, muscle is not a LTI system. In particular, motor units do not obey the principle of superposition -- that is that the response to the sum of two input sequences is not equal to the sum of the responses to the inputs separately.

The experimental work has focused on a major non-linear property of the response to neural stimulation called the catch-like effect (Burke et. al. [1970], [1976]). In this effect, very brief stimulation at a high repetition rate (even for only one interval) can cause a substantial and long-lasting enhancement of the isometric tension generated by subsequent action potential inputs. The catch-like effect is physiologically relevant in the control of fast movements because it occurs at the transient very high frequencies observed in the output of motoneurons in response to sudden

2

DEPARTMENT OF THE NAVY
OFFICE OF NAVAL RESEARCH
SEATTLE REGIONAL OFFICE
1107 NE 45TH STREET, SUITE 350
SEATTLE WA 98105-4631

IN REPLY REFER TO:

4330
ONR 247
11 Jul 97

From: Director, Office of Naval Research, Seattle Regional Office, 1107 NE 45th St., Suite 350, Seattle, WA 98105

To: Defense Technical Center, Attn: P. Mawby, 8725 John J. Kingman Rd., Suite 0944, Ft. Belvoir, VA 22060-6218

Subj: RETURNED GRANTEE/CONTRACTOR TECHNICAL REPORTS

1. This confirms our conversations of 27 Feb 97 and 11 Jul 97. Enclosed are a number of technical reports which were returned to our agency for lack of clear distribution availability statement. This confirms that all reports are unclassified and are "APPROVED FOR PUBLIC RELEASE" with no restrictions.

2. Please contact me if you require additional information. My e-mail is *silverr@onr.navy.mil* and my phone is (206) 625-3196.

ROBERT J. SILVERMAN

increases of depolarizing current (Baldissera, et. al. [1975]).

Although extensive modeling has been done of the muscle activation processes related to the phenomena illustrated by these experiments (Lehman [1982], Zahalek [1990]) little attention has been given to the catch-like non-linearity. An earlier phasic-excitation-activation (PEXA) model of the complete motor unit (Hannaford [1990]), successfully replicated many aspects of catch-like non-linear enhancement of tension development, but the model was phenomenological and did not establish a direct analogy between its state variables and biological structure.

This paper will present two new models of the muscle activation process which are more physiologically based than the corresponding portions of the PEXA model. The motor-neuron portion of the overall motor unit dynamics is not addressed here. The two models are based on storage and conduction and reaction rates of the critical ions for muscle activation, Ca^{2+} and Troponin. It will be assumed that muscle hypothetical tension (active state) is directly proportional to the amount of troponin which is doubly bound to Ca^{2+}. The two new models differ in the level of detail and by the addition of a non-linear decomposition rate function of Ca^{2+}_2Tn. The second model suggests the interpretation that the "enhancement" of tension actually represents a transition between stable equilibrium states in the reaction $2\,Ca^{2+} + Tn \longleftrightarrow Ca^{2+}_2Tn$.

Model I Description

This model of muscle activation and deactivation is based on fundamental physiological concepts and neuro-muscular physiological experimental data. The concepts of physiology involved in the model are: 1) electro-physiology, 2) diffusion and active transport, 3) chemical reaction, and 4) biomechanics. Model structure comes from these principles as they relate to release and uptake of Ca^{2+} and reaction of Ca^{2+} with Troponin. The model parameters are estimated from experimental data or, where the data are incomplete, heuristically. Also, some level of approximation is needed in order to simplify the model. (For all definitions of symbols used below, please refer to Table.1.)

The principles of this model are:

Membrane electricity: The sarcolemma and T-tubule are modeled as electrical resistors and capacitors in parallel connection (Fig.1.a). The motoneuron action potential is approximately simplified to a current impulse which transmits from axon to sarcolemma and T-tubule and deposits charge on their capacitors. The depolarization of T-tubule (V_m') is modeled as a piecewise linear function of the charge with a threshold m_{th}.

Ca^{2+} **diffusion and active transport:** Ionic calcium is stored in the sarcoplasmic reticulum

(S.R.) while muscle is resting. The transport of Ca^{2+} through S.R. membrane can be decomposed into outflow (from S.R. to sarcoplasm (S.P.)) and inflow (from S.P. to S.R.) (Fig.1.b). The inflow rate only depends on free Ca^{2+} concentration in the S.P. But the outflow rate depends on both free Ca^{2+} concentration in the S.R. and depolarization of T-tubule (V_m'). A charge deposited on the T-tubular membrane by a received action potential causes an increase in Ca^{2+} outflow conductivity for the time that it is stored by the S.R. membrane capacitance. Our model uses controlled current sources (indicated by diamonds with arrows) to represent ion transport processes (Fig.1.b) and two new elements (Fig.1.e) to represent chemical composition reactions, whose rate depends on the product of a forward rate constant and the concentration of available reactants, and decomposition reactions, whose rate depends on the product of a backward rate constant and the concentration of compounded reactants.

Activation and deactivation of contraction: Ca^{2+} in S.P. is thought to be the regulator of muscle contraction (Ebashi and Endo [1968], Aidley [1971], Gordon [1989]). Some evidence (Gordon [1989], Lehman [1982]) indicates that there are two calcium ions reacting with one receiver molecule, troponin, as the activator of contraction. This reaction is expressed in chemical equation as:

$$2\, Ca^{2+} + Tn \dashrightarrow Ca^{2+}{}_2 Tn.$$

This may be separated into two steps:

$$Ca^{2+} + Tn \dashrightarrow Ca^{2+}Tn,$$
$$Ca^{2+} + Ca^{2+}Tn \dashrightarrow Ca^{2+}{}_2 Tn.$$

Of course, both subreactions are reversible, and the equations can be rewritten as:

$$Ca^{2+} + Tn \underset{k_{n1b}}{\overset{k_{n1f}}{\longleftrightarrow}} Ca^{2+}Tn,$$

$$Ca^{2+} + Ca^{2+}Tn \underset{k_{n2b}}{\overset{k_{n2f}}{\longleftrightarrow}} Ca^{2+}{}_2 Tn.,$$

where k_{n1f} and k_{n2f} represent the forward reacting rate constants, and k_{n1b} and k_{n2b}, backward reacting rate constants (Fig.1.c).

Muscle mechanics: After the activation (two Ca^{2+} compound with a troponin), a sequence of events: 1) thin filament activation, 2) cross-bridge attachment, and 3) net-force output, occurs. these steps are approximated by a mechanical system which consists of a tension generator, a parallel damper, and a serial elastic element (Fig.1.d) as they have been used in many previous models (Huxley [1957], Aidley [1971], Hannaford [1990]).

4

Model I Equations

When an axon action potential pulse transmits to the sarcolemma and T-tubule, the membrane potential (or charge, since here the capacitance is assumed to be constant) responds as a first-order low pass filter and an exponential decay results according to the time constant of the membrane resistor and capacitor. This first order differential equation can be written:

$$\frac{d}{dt}q_m = \frac{1}{C_m}i_i - \frac{1}{R_m C_m}q_m \tag{1}$$

One way that we will deal with the large number of parameters in this model is to use normalized values for the state variables and many parameters (Table.1). Capacitance is normalized to dimensionless unit value, and resistance to units of time. Thus, each RC time constant is correctly represented in the model.

This approach is well suited to represent the dynamic aspects of muscle activation as long as nonlinear elements (below) are carefully scaled to the normalized range. The model thus predicts linear and nonlinear dynamic effects, but looses absolute amplitude information found in earlier models (Hannaford [1990]). Absolute amplitude information can be added to the model through identification of capacitance and/or resistance values and rescaling of nonlinear elements.

Applying the normalization to Equ.1 by letting $C_m == 1$, we have:

$$\frac{d}{dt}V_m = i_i - k_i V_m \tag{1.a}$$

The conductivity of outflow Ca^{2+} through the S.R. membrane is modeled as voltage-dependent channel regulated by T-tubule potential. The voltage dependence is a piecewise linear relation:

$$V_m' = (V_m - m_{th})\, u(V_m - m_{th}) \tag{2}$$

in which conductivity increases linearly with potential above a specific threshold (Aidley [1971]).

$$i_f = k_f V_m' \tag{3}$$

where $u(V_m - m_{th})$ is a unit step function of V_m with a threshold (offset) m_{th}. For example, for a short duration after an input pulse, the membrane potential will be greater than the threshold, which turns on the outflow of Ca^{2+} and increases the Ca^{2+} concentration in the S.P. .

In the opposite direction, the inflow rate of Ca^{2+} is:

$$i_b = k_b m_2 \tag{4}$$

At the same time, there is a net bidirectional reaction of Ca^{2+} in the S.R. between bound condition

and ionic condition,

$$i_s = k_s(m_0 - m_2) \tag{5}$$

driven by disequilibrium between bound and free states of Ca^{2+} in the S.R..

In the S.R. troponin compounds with Ca^{2+}. The forward and backward reaction rates for these steps are:

$$i_{n1f} = k_{n1f}m_2n_0 \tag{6}$$

$$i_{n1b} = k_{n1b}n_1 \tag{7}$$

$$i_{n2f} = k_{n2f}m_2n_1 \tag{8}$$

$$i_{n2b} = k_{n2b}n_2 \tag{9}$$

Up to this point, each node in the modeling circuit has a first order differential equation, which can be expressed as:

$$C_0\frac{dm_0}{dt} = -i_s \tag{10}$$

$$C_1\frac{dm_1}{dt} = i_s - i_f + i_b \tag{11}$$

$$C_2\frac{dm_2}{dt} = i_f - i_b - i_{n1f} + i_{n1b} - i_{n2f} + i_{n2b} \tag{12}$$

$$C_n\frac{dn_0}{dt} = -i_{n1f} + i_{n1b} \tag{13}$$

$$C_n\frac{dn_1}{dt} = i_{n1f} - i_{n1b} - i_{n2f} + i_{n2b} \tag{14}$$

$$C_n\frac{dn_2}{dt} = i_{n2f} - i_{n2b} \tag{15}$$

and by conservation of troponin (Equ.13, 14, and 15),

$$n_2 = n_{total} - n_0 - n_1 \tag{15.a}$$

The muscle activation (hypothesis tension) is simply assumed to be proportional to $[Ca^{2+}_2Tn]$ with a normalized constant of 1.

$$ht = n_2 \tag{16}$$

As a result, the dynamics for muscle mechanics is:

$$ht = B(\frac{dx}{dt}) + K(x) \tag{17}$$

We have initially linearized the muscle mechanics by assuming:

$$B(\dot{x}) = b\dot{x} \tag{18.a}$$

$$K(x) = kx \tag{18.b}$$

which gives

$$ht = b\frac{dx}{dt} + kx \tag{17.a}$$

After that, the output force, kx, is obtained.

Simulation Results of Model I

1. Response to different frequencies of pulse train inputs --

In the first simulation experiment, model I was driven by input pulse trains of different pulse rates. A similar muscle model simulation has been done by Lehman for extraocular muscle (Fig.1.18, Lehman [1982]). Four different frequency inputs (100, 250, 500, and 600 Hz) were used in that simulation. Because of the high speed of extraocular muscle, these input frequencies are too high for type S muscle fibers of the cat gastrocnemius (on the average), so, we used a lower frequency set of inputs, 8, 14, 20, and 25 Hz (Fig.2) to compare with Lehman's result. (Originally, the parameters of this model were found to best fit the experimental results of Burke et. al. [1970]. This will be discussed later. It is obvious that the muscles investigated by Burke were much slower than the extraocular muscle.)

When model I was driven by 8, 14, 20, and 25 Hz pulse trains (Fig.2), the result is very similar to Lehman's allowing for the different time scales. Typically, For each pulse input, the force response first raises up till a maximum and then falls down. If the frequency of input train is low enough, the force will tend to return to zero after it reached a maximum value for each input pulse. If the frequency goes up, the falling time will be shortened, and the amount of falling will be smaller. Thus the force keeps increasing until it saturates. If the pulse frequency is sufficient to reach saturation, the higher the frequency is, the shorter the saturation time is.

2. Response to three different patterns of pulse train inputs --

In the second simulation, three trains of input patterns were used (the same as Burke's

experiment, [1970]). Each includes 22 stimuli at a basic rate of 12.2 pulses per second (pps) (pulses interval, 82 ms). In each train, one or two stimulus intervals were altered (Fig.3). The force response traces are labeled "a", "b", and "c" separately (Fig.4), and the corresponding pulse sequences are:

"a". Starts with a pulse interval shorter than that in the basic train (10 ms). (The two pulses with a small interval are called a "doublet", and the second pulse only is called the "early pulse".)

"b". Starts with a 10 ms interval doublet (as in "a"), and the 8th pulse follows the previous pulse with an interval longer than that in the basic train (117 ms). (called the "delayed pulse")

"c". Starts without a doublet, and the 8th pulse follows the seventh pulse with an interval shorter than that in the basic train but longer than that in "a" and "b" doublet (26 ms).

Unlike the experimental data, the simulation results (Fig.4.d) do not show any prolonged enhancement. The responses corresponding to three different input patterns all approach to the same level at steady state.

Why We Need a New Model

Some enhancement was observed in the previous model because of the nonlinearity of the model, however, unlike the experimental data (Burke et. al. [1970]), the enhancement did not last. In retrospect it may be obvious that the first model can not explain the effect of enhancement lasting. In the first model, all rate coefficients are constant, therefore the force response tends to reach the same stable point if the steady state input frequency in each sequence is the same. The stable point is monotonically related to the input rate. Changing the time constants can not solve this problem, but will cause other problems such as slowing down of the increase and decrease of force response, etc. Since in this model there is only one stable response for each steady state input, the enhancement can never be lasting, no matter what transient input sequence is applied. This means that for the enhancement to prolong, there must be more than one stable point for a range of steady state inputs, and the transient input sequence will decide which stable point is approached. Based on this idea, model II involves nonconstant reacting rate coefficients in order to get two stable points.

Model II Description

Model II, like model I, can be separated into 4 stages.

Stage 1, **membrane electricity** (Fig.5.a), and stage 4, **muscle mechanics** (Fig.5.d), are exactly the same as model I.

Stage 2, **Ca^{2+} diffusion and active transport** (Fig.5.b), is almost the same but ignores the factor of bound Ca^{2+} in S.R., since this seems not to effect the lasting of enhancement. Bound Ca^{2+} in S.R. seems to play a role in tetanic contraction and Ca^{2+} recovery (Almers [1989]). It may be considered in further work, but not here.

Stage 3, **activation and deactivation of contraction** (Fig.5.c), is quite different from model I. The two-step reaction of troponin and Ca^{2+} is replaced by a simple concentration-equivalent circuit which consists of two dependent current sources. One is the composition rate of $Ca^{2+}{}_2Tn$, driven by Ca^{2+} concentration in S.P. The form of this rate dependence is a "square-saturation function" (Fig.6.a, this will be described later). The other is the decomposition rate of $Ca^{2+}{}_2Tn$, driven by $Ca^{2+}{}_2Tn$ concentration. The form of this rate dependence is approximated by a cubic spline polynomial (Fig.6.b and c) with a local maximum at P_{max} (N_1,K_1) and a local minimum at P_{min} (N_2,K_2).

An equilibrium in $Ca^{2+}{}_2Tn$ will be reached when the average composition rate equals the average decomposition rate. Since the composition rate is assumed to be independent of $Ca^{2+}{}_2Tn$, it can be visualized as a horizontal line in Fig.6.c at a given rate. Each intersection of this line with the decomposition rate curve (Fig.6.b and c) is an equilibrium point. However, only those intersections where the slope of the decomposition curve is positive are stable since at these points a small change in $Ca^{2+}{}_2Tn$ concentration will be corrected by the resulting change in decomposition rate. Thus, for composition rates, K, between K_2 and K_1, the decomposition rate function has three equilibria: 2 stable ones, SP_1 (N_4,K) and SP_2 (N_6,K), and a unstable one, P_{crt} (N_5,K).

When a regular impulse train arrives at the T-tubule, if 1), the firing rate is lower than a threshold frequency, the average composition rate of $Ca^{2+}{}_2Tn$ in each pulse duration will be less than the average decomposition rate K_1 (Fig.6.c) at $[Ca^{2+}{}_2Tn] = N_1$. Thus the stable point for $[Ca^{2+}{}_2Tn]$ is at the left side of N_1. If 2), the firing rate is greater than the threshold, the average composition rate will be greater than the average decomposition rate K_1 at $[Ca^{2+}{}_2Tn] = N_3$. Thus the stable point for $Ca^{2+}{}_2Tn$ is at the right side of N_3.

On the other hand, when 3) an impulse train contains a doublet (one impulse duration much shorter than the others) and the main firing rate is just a little lower than the threshold, the average compounding rate K for the main firing rate will be less than the average decomposition rate K_1 but greater than K_2. Before the doublet, the force response will be all the same as in 1), on the left side of N_1, at SP_1 (N_4,K). But at the doublet, it may be pushed across the local maximum P_{max} (N_1,K_1), further more, across the critical point P_{crt} (N_5,K) (in the view of short-term average).

9

After that, it will reach another stable point SP_2 (N_6,K), between N_2 and N_3. This keeps Ca^{2+}_2Tn concentration at a new level greater than the one without doublet input.

Furthermore, consider that the input is similar to 3) but after the doublet there is one delayed impulse (duration longer than the others). Before the delayed impulse, the response will be all the same as in 3). And if 4) the delay is not too long, the average composition rate will not decline below K_2 and after the delayed impulse the response may still be kept in the right side of P_{crt}, and gradually comes back to SP_2. But if the delay is long enough, after the delayed impulse, it may be pulled back to the left of P_{crt} (in the view of short-term average), and returns to the lower stable level SP_1.

Model II Equations

For all definitions of symbols used below, please refer to Table.1 and Table.2.

In this model, the differential equation of sarcolemma and T-tubule membrane potential (or charge) is exactly as in model I:

$$\frac{d}{dt}V_m = i_i - k_i V_m \tag{1.a}$$

The voltage dependence of the Ca^{2+} inflow through S.R. membrane and the Ca^{2+} outflow are also the same:

$$V_m' = (V_m - m_{th})\, u(V_m - m_{th}) \tag{2}$$

$$i_f = k_f V_m' \tag{3}$$

$$i_b = k_b m_2 \tag{4}$$

However, the composition rate of Ca^{2+}_2Tn is now modeled as:

$$i_{nf} = k_n F(m_2) \tag{19}$$

where

$$F(m_2) = \frac{m_2^2}{m_2^2 + M} \tag{20}$$

is the normalized composition rate function. Similarly, the decomposition rate of Ca^{2+}_2Tn:

$$i_{nb} = k_n G(n) \tag{21}$$

10

where

$$G(n) = Spline(X, Y)(n) \tag{22}$$

and "$Spline(X,Y)(n)$" is a cubic Spline polynomial, determined by a set of predetermined points (Table.3), with respect to variable n.

As a result, the dynamic equations are:

$$C_1 \frac{dm_1}{dt} = -i_f + i_b \tag{23}$$

$$C_2 \frac{dm_2}{dt} = i_f - i_b \tag{24}$$

$$C_n \frac{dn}{dt} = i_{nf} - i_{nb} \tag{25}$$

The muscle mechanics are the same as model I but n_2 is replaced by n:

$$ht = n \tag{26}$$

$$ht = B(\frac{dx}{dt}) + K(x) \tag{17}$$

or

$$ht = b\frac{dx}{dt} + kx \tag{17.a}$$

Simulation Results of Model II

1. Response to different frequencies of pulse train inputs --

Model II was driven by constant frequency pulse trains using the same frequencies as used in model I (Fig.7). In general, the force responses are very similar to the results of both model I and Lehman's model [1982]. But, looking at the data in more detail, there is a difference in the low frequency components of the force response. In model I, the response is like a simple exponential saturation behavior, its rate of increase decreases as force rises; in model II, it isn't so simple, the rate of increase seems to decrease, increase, and decrease again as force rises (especially for frequency = 14 Hz). This is also true of Lehman's model [1982] (frequency = 500 Hz).

2. Response to three different patterns of pulse train inputs --

In contrast to model I, the responses of model II (Fig.8) to the three pulse trains "a", "b", and "c" show significant enhancement of tension for trains "a", and "b" due to their initial doublets, and no crossing of the force traces. The initial effect of the doublet is greater than the increase caused by the later short interval (of longer duration) in train "c". These features are all consistent with the experimental data (Burke et. al. [1970]).

3. Response to input trains with or without doublet --

These simulations (Fig.9) are similar to the previous ones, but instead of three different patterns, only two pulse trains are used as inputs: one with a 10 ms doublet at the beginning and the other without. Several frequencies of the basic train were selected (1, 8, 12, 20 Hz) based on earlier experimental data (Burke et. al. [1970]).

The simulations show significant early enhancement of tension in response to the trains containing the doublet for all frequencies tested. The enhancement is maintained for a duration which varies with the basic pulse train rate: i.e. about 0.8 second at 8 Hz, greater than 1.6 second at 12 Hz, and about 0.4 second at 20 Hz.

Prediction of Model II

As described in "Model II Description" section, two phenomena are expected:

1. If originally the force response was around the higher force stable point, and an input pulse interval is increased more than a certain amount, τ_1, this will result in pulling the force response down to the lower force stable point.

2. If originally the force response was around the lower force stable point, and an input pulse interval is shorter than a certain amount, τ_2, this will result in pushing the force response up to the higher force stable point. If the interval is shortened, but still longer than τ_2, the force will temporarily increase but go back to the lower force stable point.

Model II was driven by 82 ms pulse trains with a doublet at the beginning resulting in steady state force at the high equilibrium point, each containing an interval delayed by 35, 50, 75, 100, and 200 ms (Fig.10.a), and by pulse trains without a doublet at the beginning resulting in steady state force at the low equilibrium point, each containing an interval reduced to 26, 30, 37, 47, and 67 ms (Fig.10.b).

From the high equilibrium point (SP$_2$), intervals delayed by more than 75 ms resulted in

changing the system to SP_1 (Fig.10.a). Thus the value of τ_1 should be somewhere between 75 ms and 100 ms. From the low equilibrium point (SP_1), intervals shorter than 37 ms resulted in changing the system to SP_2 (Fig.10.b). Thus the estimated value of τ_2 should be between 30 ms and 37 ms.

Discussion

We have presented two new models of muscle activation, expressed as circuit diagrams, mathematical equations, and computer simulations.

Models

Model I, although not as detailed as that of Lehman [1982], contains most of the reactions thought to be involved in binding of Ca^{2+} to troponin for the activation of muscle force generators. These include S.R. membrane electrical properties, bound and free Ca^{2+} in the S.R., Ca^{2+} transport across the S.R. membrane, and the two stage formation of Ca^{2+}_2Tn.

Model I was good at reproduction of the development and relaxation of tension (Fig.2), but although it showed some enhancement of tension, it could not reproduce the qualitative features of the responses to the doublet/gap stimulation paradigms found by Burke et. al. [1970] (Fig.4.d). In particular, the enhancement due to the initial doublet (traces "a", "b") was insufficient to prevent a later doublet (trace "c") from causing the force trajectories to cross.

Although it might be possible to prove that significant enhancement is possible with the structure of model I due to its significant nonlinearities, we could not find a set of parameter values which could produce this behavior and such a proof was not obvious.

A second model was described which introduced at the same time a simplification and an elaboration of Model I. The main simplification was to lump the two-step reaction of the formation of Ca^{2+}_2Tn into a single step characterized by composition and decomposition rate functions and to lump the two states of Ca^{2+} in the S.R. into one. The elaboration was the introduction of two nonlinear functions describing Ca^{2+}_2Tn composition as a function of free Ca^{2+} concentration in the S.P. (m_2), and Ca^{2+}_2Tn decomposition as a function of Ca^{2+}_2Tn concentration (n).

The composition rate function for Ca^{2+}_2Tn is a second order rational polynomial with saturation indicating a maximum composition rate. This curve (similar to the logistic curve) illustrates a fundamental nonlinear dynamic relationship in which rate of change depends on state, but the state is limited by a maximum extent (such as a "limit to growth" in population systems). The composition rate function used here (Equ.20) is similar to the "activation factor" used by

13

Zahalek [1990] to couple Ca^{2+} to cross-bridge dynamics. While the composition rate function is in a slightly different place in the reaction, it may produce a qualitatively similar effect.

The second non-linear function (described by anchor points and a cubic spline) which describes the rate of decomposition of Ca^{2+}_2Tn, had a region of negative slope which caused the existence of two stable points in Ca^{2+}_2Tn concentration for a given steady state input frequency. The existence of two stable points only occurs within a range of Ca^{2+}_2Tn concentrations.

Within this range, the combined effect of these two curves is to give two possible steady state force responses for a given input rate, a "normal" response at the lower equilibrium point, and an "enhanced" response at the higher point. A single interval, if sufficiently shortened relative to the basic pulse rate, can push the system from the normal to the enhanced response, and a single interval sufficiently lengthened relative to the basic rate can push the system from the enhanced to the normal response.

A possible source of the nonlinear composition and decomposition rate functions may be the effect of interaction between Ca^{2+} mobility and polarization induced by intercellular proteins (Ling [1991]).

Simulations

In response to the basic pulse train inputs (Fig.7), model II gave traces of force development which were similar in shape at first glance to those of model I. The saturation level was higher, and it was reached faster for the high frequency inputs. However, an interesting qualitative effect appears when the 14 Hz trace is viewed along its direction, near the plane of the page. The rate of increase can be seen to oscillate slightly. This is clearly due to the system passing through the non-monotonicity of Ca^{2+}_2Tn decomposition curve (Fig.6.b and c) as tension is increased. Although this curve is not explicitly represented in Lehman's model, the oscillations in force development can also be observed in his simulation (Fig.1.18, Lehman [1982]). He did not perform simulations to demonstrate catch-like enhancement in his model, but this similarity suggests that it should be observed.

The doublet/delay experiment (traces "a", "b", "c", Fig.3) was devised by Burke et. al. [1970] to elucidate the nonlinear nature of the catch-like property and its decay. The different responses to these three input signals clearly distinguished the two models (Fig.4 vs. Fig.8). In particular, the declining level of average force seen in the doublet responses of model II (traces "a" and "b", Fig.8.c) was not observed in the output of Model I to the same stimulus. This was due to the lack of a strong doublet effect in Model I. In model II, the initial doublet pushed the system past the "enhanced" stable point, SP_2, and the extended interval (trace "b", Fig.8.c) caused force level to temporarily decline, but was not extended by enough extra time to make the system drop to the

"normal" stable point, SP_1.

The nonlinear decomposition rate function was seen to result in two stable operating points, but only if the steady state composition rate was sufficient to generate a Ca^{2+}_2Tn composition rate within the interval in which a horizontal line will intersect the decomposition rate curve at three points. This suggests that significant enhancement should only be seen for basic pulse train rates which are intermediate between very low stimulation and very high stimulation.

The dual pulse step experiments (Fig.9.a-d) were used by Burke et. al. [1976] to quantify this behavior in the living muscle. Burke's results showed enhancement for each of the basic pulse train rates, but the duration of the enhancement was variable. Our simulations using model II (Fig.9.a-c) show the same behavior which can be interpreted in terms of the dual stable state hypothesis of model II. For all cases, the initial doublet is sufficient to push the system past critical point P_{crt}. However, for the pulse rates below about 12 Hz, the steady state composition rate is below the level at which two stable points exist, K_2, the system is forced to a single point, and the traces converge in less than 1 second (Fig.9.a, and b) for intermediate intervals (for example 12 Hz, Fig.9.c) the composition rate is between the critical values, K_2 and K_1, and the enhancement is long lasting. For the highest pulse rate, (20 Hz, Fig.9.d) the basic pulse rate is sufficient to drive the system above K_1, and thus there is a single stable point to which both traces converge. This behavior is consistent with the experimental data (Figure 5, Burke et. al. [1976]).

A significant issue is whether or not the enhancement ever disappears if the input is continued at an appropriate rate. It is interesting to note that the stimulus trains of Burke et. al. [1976] lasted for about 1.6 seconds and that for intermediate frequencies 9.8 - 15 Hz, the traces do not converge. Additional experimentation is needed to determine if there are indeed two permanent stable states, or whether they eventually converge. Our model suggests that the effect is permanent baring effects due to fatigue etc.

Predictions

The dual stable point idea of model II prompted us to generalize the abc experimental input stimuli of the Burke experiment to a larger number of doublet intervals and increased gap intervals, and to start the system from both the "enhanced" state (Fig.10.a) and the "normal" state (Fig.10.b). These simulations suggest that further experimental work can determine the stable points SP_1 and SP_2, and the additional pulse delay (τ_1) which will cause the transition from SP_1 to SP_2. Our model, which is tuned to fit the Burke data, suggests that in the slow motor units of cat medial gastrocnemius muscle, this interval should be between 75 and 100 ms. if the basic input rate is 12.2 Hz.

The other suggested experiment is to identify a reduced interval length which will cause the

15

system to transition from the "normal" (SP_1) to the "enhanced" (SP_2) stable point. Our prediction is that this interval will be between 37 and 30 ms in this muscle for the 12.2 Hz basic rate.

Limitations and Future Work

Model II developed a satisfactory explanation for the catch-like property of muscle, but at the cost of the substitution of abstract composition and decomposition functions for detailed chemical reaction modeling. Lehman's model [1982] is a quite detailed model which includes additional steps involved in the composition and decomposition of Ca^{2+}_2Tn. Model II contains three state variables and two non-linear composition and decomposition functions. The similarity between the non-uniform force development rate in our model and Lehman's is a suggestion that Lehman's model may contain this phenomenon.

A future step will be to test the model in non-isometric experiments. One significant issue will be the extent to which muscle mechanical variables affect activation level. The existence of such a feedback loop, which is not present in our models, has been suggested by Zahalek's tight coupling hypothesis [1990], and can be observed in other systems such as insect flight muscle (Pringle [1949]). Whether and how such mechanical feedback loops may effect the stable states of contraction remains to be determined.

References

Aidley, D.J., "The Neuromuscular Junction", in The Physiology of Excitable Cells, Chapter 6, 1971.

Aidley, D.J., "The Organization of muscle cells", in The Physiology of Excitable Cells, Chapter 11, 1971.

Aidley, D.J., "The Dynamics of Muscular Contraction", in The Physiology of Excitable Cells, Chapter 12, 1971.

Almers, W., "Excitation-Contraction Coupling in Skeletal Muscle", in Textbook of Physiology, vol. 1: Excitable Cells and Neurophysiology, Chapter 7, 21st edition, Seattle, Washington, 1989.

Baldissera, F. and Parmiggiani, F., "Relevance of Motoneuronal Firing Adaptation to Tension Development in the Motor Unit", Brain Research, vol. 91, 315-320, 1975.

Burke, R.E., Rudomin, P., and Zajac, F.E., "Catch Property in single Mammalian Motor Units", Science, vol.168, 122-124, 1970.

Burke, R.E., Rudomin, P., and Zajac, F.E., "The Effect of Activation History on Tension Production by Individual Muscle Units", Brain Research, vol. 109 515-529, 1976.

Ebashi, S. and Endo, M., "Calcium Ion and Muscle Contraction", Progress in Biophysics & Molecular Biology, vol. 18, 123-183, 1968.

Gordon, A.M., "Molecular Basis of Contraction", in Textbook of Physiology, vol. 1: Excitable Cells and Neurophysiology, Chapter 8, 21st edition, Seattle, Washington, 1989.

Gordon, A.M. "Contraction in Skeletal Muscle", in Textbook of Physiology, vol. 1: Excitable Cells and Neurophysiology, Chapter 9, 21st edition, Seattle, Washington, 1989.

Gordon, A.M., "Contraction in Smooth Muscle and Nonmuscle Cells", in Textbook of Physiology, vol. 1: Excitable Cells and Neurophysiology, Chapter 10, 21st edition, Seattle, Washington, 1989.

Gurfinkel, V.S. and Levik, Y.S., "Effects of Doublet or Omission and Their Connexion with the Dynamics of the Active State of Human Muscles", Problems of Information Transmission, U.S.S.R. Academy of Sciences, Moscow, May, 1974.

Hannaford, B. and Stark, L., "Roles of the Elements of the Tri-Phasic Control Signal", Experimental Neurology, vol. 90, 619-634, 1985.

Hannaford, B., Kim, W.S., Lee, S.H., and Stark, L., "Neurological Control of Head Movements: Inverse Modeling and Electromyographic Evidence", Math. BioScience, vol. 78, 159-178, 1986.

Hannaford, B. and Stark, L., "Late Agonist Burst (PC) Required for Optimal Head Movement: a Simulation Study", Biological Cybernetics, vol. 57, 321-330, 1987.

Hannaford, B., "A Nonlinear Model of the Phasic Dynamics of Muscle Activation", IEEE Trans Biomedical Engineering, 1990.

Hodgkin, A.L. and Huxley, A.F., "A Quantitative Description of Membrane Currents and its Application to Conduction and Excitation in Nerve", J. Physiol., vol. 117, 500-544, 1952.

Huxley, A.F., "Muscle Structure and Theories of Contraction", 1957.

Lehman, S.L. "A Detailed Biophysical Model of Human Extraocular Muscle", Dissertation of Doctor of Philosophy in Biophysics of the University of California, Berkeley, 1982.

Ling, G., "A Revolution in the Physiology of the Living Cell: and Beyond", 1991.

Pollack, G.H., "Muscles & Molecules: Uncovering the Principles of Biological Motion", Seattle, Washington, 1990.

Pringle, J., "The Excitation and Contraction of the Flight Muscles of Insects", J. Physiol., vol. 149, 29-30, 1949.

Zahalek, G, "Modeling Muscle Mechanics", in Multiple Muscle Systems, ed J. Winters and S. Woo, Springer Verlag, 1990.

Legend

Fig.1

Equivalent circuits of first model of muscle activation (model I): a) Muscle membrane electricity. b) Ca^{2+} diffusion and active transport between sarcoplasmic reticulum (S.R.) and sarcoplasm (S.P.). c) Activation and deactivation. The node voltage is equivalent to ionic or molecular concentration; branch current to ion flow; capacitance to equivalent ionic or molecular distribution volume; conductance to diffusive constance; and dependent current source to active transport. e) Two defined symbols, chemical composition reaction and decomposition reaction, are used in c), which are similar to dependent current sources but with dependence on the product of rate constants and the concentration of the reactants (the inputs). d) Muscle mechanics. The output tension of the tension generator is modeled as proportional to the output of c).

Fig.2

Model I output force in response to four fixed frequencies of pulse train inputs.

Fig.3

Three patterns of pulse trains used as simulation inputs. The main frequency of all three patterns is 12.2 Hz, or pulses per second (pps) (duration 82 ms). Sequence a (symbol x) has a 10 ms doublet in the beginning. Sequence b (symbol *) has a 10 ms doublet in the beginning but a 35 ms delayed pulse (duration is 117 ms) after the 7th pulse. Sequence c (symbol o) has a 26 ms doublet at the 7th pulse.

Fig.4

Response of model I for the three different input patterns of Fig.3: solid line, sequence "a"; dashed line, sequence "b"; dotted line, sequence "c". a) Ca^{2+} concentration. b) $Ca^{2+}Tn$ concentration. c) Ca^{2+}_2Tn concentration. The hypothetical tension is proposed to be proportional to $[Ca^{2+}_2Tn]$. d) Output force (isometric). All three traces approach the same steady state as long as the frequencies of the main pulse trains are the same. There is no way to get a prolonged enhancement with model I, no matter how the model parameters change.

Fig.5

Equivalent circuits of model II: a) and d), membrane electricity and muscle mechanics, are exactly the same as model I. b) Ca^{2+} diffusion and active transport is similar to model I but without C_0, m_0, and k_s. c) activation and deactivation. The composition rate and decomposition rate are modeled as two nonlinear dependent current sources respectively without considering of the complexity of chemical reaction.

Fig.6

a) Composition rate as a function of $[Ca^{2+}]$. b) Decomposition rate as a function of $[Ca^{2+}_2Tn]$. c) The detail of decomposition curve as described in text.

Fig.7

Model II output force in response to pulse train inputs of four fixed frequencies. View the response 14 Hz from the direction of the eye's icon to see the change of force increase rate due to added nonlinear element (see text for detail).

Fig.8

Response of model II for the three different input patterns: solid line, sequence "a"; dashed line, sequence "b"; dotted line, sequence "c". a) Ca^{2+} concentration. b) Hypothetical tension. c) Output force. This result is very similar to the experimental results made by Burke et. al., 1970. Prolonged enhancement is obvious.

Fig.9

Response of model II for doublet experiments: a) 1 pps, b) 8 pps, c) 12 pps, and d) 20 pps. These results are also very similar to the experimental results made by Burke et. al., 1970.

Fig.10

a) Output force for prediction 1. Input pattern is similar to sequence b in Fig.3, but with five different delay times. If the pulse is delayed by more than a certain amount (here, 75 ms), the output force will be pulled back to low tension stable region. b) Output force for prediction 2. Input pattern is similar to sequence c in Fig.3, but with five different doublet intervals. If the doublet interval is wider than a certain amount (here, 30 ms), the output force will not be pushed to its high tension stable region.

Symbol definitions of model I

1. Membrane electricity:

Name	Type*	Value†	Unit‡	Description
i_{in}	I	1 or 0	1/sec	Unit impulse, the current of action potential
C_m	C	1	-	sarcolemma and T-tubular capacitance
R_m	C	0.01	sec	sarcolemma and T-tubular resistance
q_m	SV	-	-	sarcolemma and T-tubular charge
V_m	SV	-	-	sarcolemma and T-tubular potential
V_m'	CV	-	-	Ca^{2+} channel voltage dependence
m_{th}	C	0.4	-	S.R. membrane threshold for outflow Ca^{2+}
k_i	C	100	1/sec	reciprocal of $R_m C_m$

2. Ca^{2+} diffusion and active transport:

Name	Type	Value	Unit	Description
m_{total}	C	1000	-	total Ca^{2+} of S.R. under resting
m_0	SV	-	-	bound Ca^{2+} concentration in S.R.
m_1	SV	-	-	free Ca^{2+} concentration in S.R.
m_2	SV	-	-	free Ca^{2+} concentration in S.P.
C_0	C	0.9	-	bound Ca^{2+} equivalent volume in S.R.
C_1	C	0.1	-	free Ca^{2+} equivalent volume in S.R.
C_2	C	1.0	-	free Ca^{2+} equivalent volume in S.P.
i_s	CV	-	1/sec	bound-free transient rate of Ca^{2+} in S.R.
i_f	CV	-	1/sec	outflow rate of Ca^{2+}
i_b	CV	-	1/sec	inflow rate of Ca^{2+}
k_s	C	0.5	1/sec	i_s rate constant
k_f	C	50	1/sec	i_f rate constant
k_b	C	450	1/sec	i_b rate constant

Table.1-1

3. Activation and deactivation of contraction:

Name	Type	Value	Unit	Description
n_{total}	C	5	-	total Tn
n_0	SV	-	-	Tn concentration
n_1	SV	-	-	Ca^{2+}Tn concentration
n_2	SV	-	-	Ca^{2+}_2Tn concentration
C_n	C	10	-	equivalent volume of total troponin
i_{n1f}	CV	-	1/sec	forward reacting rate of step 1
i_{n1b}	CV	-	1/sec	backward reacting rate of step 1
i_{n2f}	CV	-	1/sec	forward reacting rate of step 2
i_{n2b}	CV	-	1/sec	backward reacting rate of step 2
k_{n1f}	C	50	1/sec	i_{n1f} rate constant
k_{n1b}	C	100	1/sec	i_{n1b} rate constant
k_{n2f}	C	5	1/sec	i_{n2f} rate constant
k_{n2b}	C	200	1/sec	i_{n2b} rate constant

4. Muscle mechanics:

Name	Type	Value	Unit	Description
k	C	1	-	equivalent muscle serial elasticity
b	C	0.15	sec	equivalent muscle parallel damping
ht	CV	-	-	muscle hypothetical tension
x	O	-	-	muscle decremental distance

Note: * The types of symbols: †‡ All values and units used for model simulation
          I: input variable   are normalized.
          SV: state variable
          CV: calculating variable
          O: output variable
          C: constant

Table.1-2

Symbol definitions of model II

1. Membrane electricity:

(same as model I, but some values of constants are changed as following)

Name	Type	Value	Unit	Description
R_m	C	0.00909	sec	sarcolemma and T-tubular resistance
k_i	C	110	1/sec	reciprocal of $R_m C_m$

2. Ca^{2+} diffusion and active transport:

(similar to model I without m_{total}, m_0, C_0, i_s, and k_s, also, some values of constants are changed as following)

Name	Type	Value	Unit	Description
m_1	C	1000	-	Ca^{2+} concentration in S.R.
C_1	C	∞	-	free Ca^{2+} equivalent volume in S.R.
C_2	C	1	-	free Ca^{2+} equivalent volume in S.P.
k_f	C	10	1/sec	i_f rate constant
k_b	C	90	1/sec	i_b rate constant

Table.2-1

3. Activation and deactivation of contraction:

Name	Type	Value	Unit	Description
n	SV	-	-	Ca^{2+}_2Tn concentration
C_n	C	1	-	equivalent volume of total troponin
M	C	500	-	$[Ca^{2+}]^2$ at half Ca^{2+}_2Tn-composition-rate
i_{nf}	CV	-	1/sec	Ca^{2+}_2Tn compounding rate
i_{nb}	CV	-	1/sec	Ca^{2+}_2Tn decomposing rate
k_n	C	52	1/sec	$F(m_2)$ and $G(n)$ modified ratio

4. Muscle mechanics:

(same as model I, but constant b is changed as following)

Name	Type	Value	Unit	Description
b	C	0.04	sec	equivalent muscle parallel damping

Table.2-2

8 control points of spline polynomial

X	Y
0.00	0.000
0.10	0.030
0.20	0.043
0.30	0.043
0.40	0.041
0.50	0.042
0.60	0.048
1.00	1.000

X : Normalized Ca^{2+}_2Tn concentration
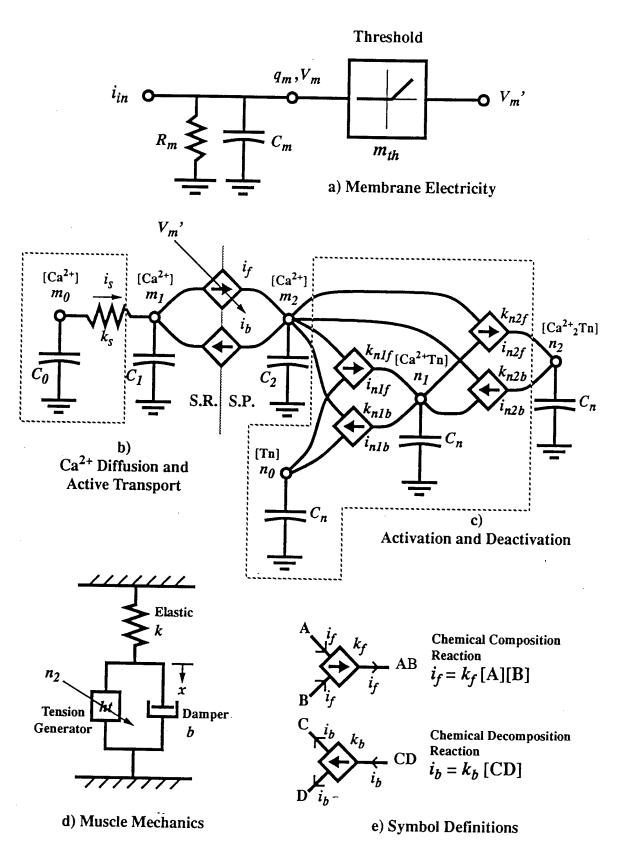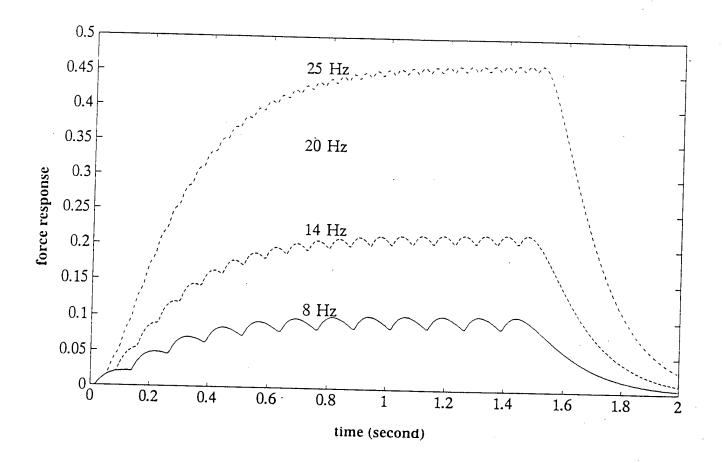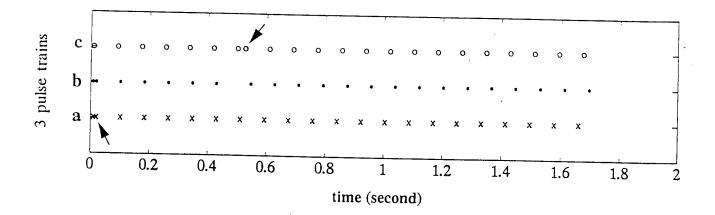Y : Normalized Ca^{2+}_2Tn decomposition rate

Table.3
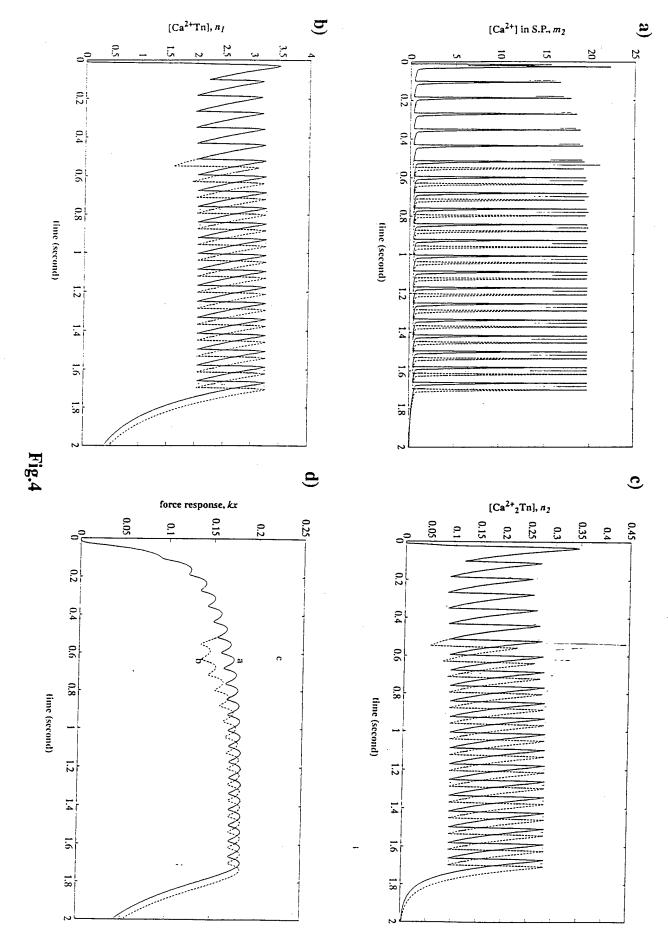
Threshold

i_{in} q_m, V_m $V_m{}'$

R_m C_m m_{th}

a) Membrane Electricity

$V_m{}'$

$[Ca^{2+}]$ i_s $[Ca^{2+}]$ i_f $[Ca^{2+}]$ k_{n2f} $[Ca^{2+}{}_2Tn]$

m_0 m_1 m_2 i_{n2f} n_2

i_b k_{n1f} $[Ca^{2+}Tn]$ k_{n2b}

k_s i_{n1f} n_1 i_{n2b}

C_0 C_1 C_2 k_{n1b} C_n

S.R. | S.P. i_{n1b} C_n

b)
Ca^{2+} Diffusion and
Active Transport

$[Tn]$
n_0

C_n

c)
Activation and Deactivation

Elastic
k

n_2

x

Tension
Generator ht Damper
   b

d) Muscle Mechanics

A i_f k_f Chemical Composition
       AB   Reaction
B i_f i_f $i_f = k_f\,[A][B]$

C i_b k_b Chemical Decomposition
       CD   Reaction
D i_b i_b $i_b = k_b\,[CD]$

e) Symbol Definitions

Fig.1

Fig.2

Fig.3

Fig.4

Threshold

a) Membrane Electricity

b) Ca^{2+} Diffusion and
Active Transport

c) Activation and Deactivation

d) Muscle Mechanics

Fig.5

a) [Ca²⁺₂Tn composition rate, $F(m_2)$ vs [Ca²⁺] in S.P., m_2]

b) [Ca²⁺₂Tn decomposition rate, $G(n)$ vs [Ca²⁺₂Tn], n]

c) [Ca²⁺₂Tn Decomposition Rate, $G(n)$ vs Ca²⁺₂Tn Concentration, n]

Fig.6

Fig.7

Fig.8

Fig.9

33

Fig.10